Article

State of Charge Estimation for Lithium-Ion Power Battery Based on H-Infinity Filter Algorithm

Lan Li [1], Minghui Hu [1,*], Yidan Xu [1], Chunyun Fu [1,*] , Guoqing Jin [2] and Zonghua Li [2]

[1] State Key Laboratory of Mechanical Transmissions, School of Automotive Engineering,
    Chongqing University, Chongqing 400044, China; lilan@cqu.edu.cn (L.L.); 20173202022t@cqu.edu.cn (Y.X.)
[2] Chongqing Changan Automobile Co., Ltd., Chongqing 400023, China; jingq@changan.com.cn (G.J.);
    Lizh3@changan.com.cn (Z.L.)
* Correspondence: hu_ming@cqu.edu.cn (M.H.); fuchunyun@cqu.edu.cn (C.F.)

check for updates

Abstract: To accurately estimate the state of charge (SOC) of lithium-ion power batteries in the event of errors in the battery model or unknown external noise, an SOC estimation method based on the H-infinity filter (HIF) algorithm is proposed in this paper. Firstly, a fractional-order battery model based on a dual polarization equivalent circuit model is established. Then, the parameters of the fractional-order battery model are identified by the hybrid particle swarm optimization (HPSO) algorithm, based on a genetic crossover factor. Finally, the accuracy of the SOC estimation results of the lithium-ion batteries, using the HIF algorithm and extended Kalman filter (EKF) algorithm, are verified and compared under three conditions: uncertain measurement accuracy, uncertain SOC initial value, and uncertain application conditions. The simulation results show that the SOC estimation method based on HIF can ensure that the SOC estimation error value fluctuates within ±0.02 in any case, and is slightly affected by environmental and other factors. It provides a way to improve the accuracy of SOC estimation in a battery management system.

1. Introduction

The state of charge (SOC) estimation is the most basic function of battery status monitoring. SOC represents the remaining power of the battery, and accurate SOC estimations are of great significance in improving the battery efficiency and safety performance [1,2]. Currently, domestic and foreign scholars have been researching different SOC estimation methods for lithium-ion batteries, which can be divided into four major categories [3]: estimation methods based on characteristic parameters of lithium-ion batteries, estimation methods based on ampere-hour integration, data-driven estimation methods, and model-based estimation methods.

The derivation process of SOC estimation for lithium-ion batteries involves many characteristic parameters, such as open circuit voltage (OCV), residual capacity, and electrochemical impedance. There is a certain mapping relationship between these characteristic parameters and SOC. The latter can be estimated by establishing this mapping relationship. The method of obtaining the battery residual capacity by a discharge test is considered to be the most direct method to determine the SOC value of lithium-ion batteries [4]. In addition to using the current residual capacity as a parameter, M. Einhorn et al. [5] used a linear interpolation method to estimate the battery's SOC based on the functional relation curve between the SOC and OCV. However, this type of method can only be applied under specific environmental constraints, such as laboratories, since it is impossible to carry out long-term constant current discharges or static states during the motion of electric vehicles.

Therefore, characterization parameters such as residual capacity and OCV cannot be determined [6,7]. A. J. Salkind et al. [8] optimized the parameters of the established fuzzy model through experimental data. This fuzzy model can fit the relationship between the battery charge state and electrochemical impedance spectroscopy (EIS) values, and the estimated error of the SOC can be controlled within 5%. However, online measurement of EIS is not easy, and varies with battery type and experimental conditions. The exact relationship between EIS and SOC and the repeatability of the online measurement of EIS needs to be studied further.

The ampere-hour integration [9], also known as the coulomb counting method, incurs a low calculation cost, as well as enables fast calculation. It is the estimation method of the SOC currently adopted by most electric vehicles. However, the estimation method based on ampere-hour integration requires high accuracy requirements from the initial parameters of the battery model. It is difficult to meet the sampling accuracy and frequency requirements of the sensor during the actual application of the battery.

Data-driven estimation methods can be divided into three categories according to different algorithms: support vector machine (SVM) [10], neural network (NN) [11], and the fuzzy control method [12]. These methods are similar to the black box model in the battery modeling process. In order to achieve high estimation accuracy and strong adaptability, a large amount of data is usually required for training. Moreover, the selection of training data is very strict, while requiring high precision in data fitting, as well as meeting the applicability of non-linear models. The data that does not meet the requirements will make it difficult to train the model, which will affect the accuracy and, consequently, the SOC estimation to a great extent.

The model-based SOC estimation method is self-adjusted by the difference between the battery's measured voltage and the model's output voltage. This is done to overcome the error caused due to uncertainty, and achieve the purpose of improving the estimation accuracy of the SOC. It is a robust closed-loop estimation algorithm. Common methods include the impedance method [13], particle filter (PF) [14], Kalman filter (KF) [15], and improved algorithm [16–18]. Among them, the PF algorithm can provide better results in a non-Gaussian white noise system, but its operation intensity is higher than that of the KF algorithm. The KF algorithm is widely used, because it can find the optimal solution for a linear Gaussian system. A simple linear system can use the ordinary KF algorithm [19], whereas for complex nonlinear models, the extended Kalman filter (EKF) algorithm has been studied and applied extensively [20–22]. Based on the equivalent circuit model, Plett [23,24] used Kalman filter series algorithms (KF, EKF, unscented Kalman filter (UKF)) to achieve the identification of model parameters and SOC estimation at the same time. Sun et al. [25] improved the traditional EKF algorithm, and realized that when the input and output of the system changed, the noise covariance matrix in the algorithm responded accordingly to self-correct the noise. Thus, the influence of noise on the accuracy of the traditional EKF algorithm is overcome; however, the EKF algorithm requires that the input noise of the model be white noise with known statistical characteristics. It is greatly affected by the measurement accuracy of the sensor during vehicle operation, and has not been applied in real vehicles.

To solve the above problems, the H-infinity filter (HIF) algorithm based on the minimum-maximum criterion is adopted in this study instead of the traditional EKF algorithm. This algorithm takes into account the time-varying element of battery parameters, and does not require the details of process noise and measurement noise. Therefore, the HIF can expand the scope of application of the SOC estimation algorithm and improve the robustness of the algorithm under real vehicle operating conditions. Chen et al. [26] used the HIF algorithm to estimate the SOC of lithium-ion batteries, and the method was tested by real-time experimental data of batteries. However, it ignores the measurement noises and random disturbances. Shu et al. [27] proposed an adaptive H-infinity filter (AHIF) algorithm to predict the SOC of lithium-ion batteries. The proposed algorithm is comprehensively validated within a full operational temperature range of battery, and with different aging status. Even so, it ignores the effects of application conditions on SOC estimation. In [28–30], the HIF is also applied to the

model parameters identification and state estimation. The results show that it has better performance than UKF and EKF. However, none of the above algorithms comprehensively analyze the influence of various uncertain factors (i.e., noises, SOC initial value, and application conditions) on the SOC estimation results of lithium-ion batteries.

To explore the influence of different uncertainties (i.e., noises, SOC initial value, and application conditions) on the estimation results when HIF is used for SOC estimation, the following chapters of this paper are arranged as follows. In the second part, a fractional-order battery model of the lithium-ion battery is established. The hybrid particle swarm optimization (HPSO) algorithm based on a genetic crossover is used to identify the parameters of the built model to obtain the initial values of the model parameters. The accuracy of the model parameter identification under different working conditions is also verified. In the third part, the HIF based on the minimum-maximum criterion is proposed to estimate the SOC of the lithium-ion battery. The robustness of the algorithm is verified under three conditions: uncertain measurement accuracy, uncertain initial value of SOC, and uncertain application conditions. Hereafter, we compared the SOC estimation results obtained using the EKF algorithm. The fourth part presents the conclusion of the article.

2. Establishment of Fractional-Order Model and Parameter Identification

The establishment of an effective battery model is the premise and foundation for studying battery SOC. Lower model accuracy will directly reduce the precision of the SOC estimation algorithm, and even directly lead to the divergence of the estimation algorithm in serious cases. From the perspective of EIS, a circuit composed of fractional components can better fit the impedance characteristics of the battery, so that they can be applied in battery principle analysis, model establishment, and state estimation [31].

2.1. Establishment of Fractional-Order Model

According to the detailed analysis of EIS in [32], this study established the fractional-order equivalent circuit model of a lithium-ion battery, as shown in Figure 1. R_0 represents the Ohmic internal resistance of the battery, R_1 and R_2 are the pure resistive impedance, CPE stands for the constant phase element, and W represents the Warburg element. The terminal voltage and OCV of the battery are represented by U_d and U_{ocv}, respectively, and I is the current value of the circuit.
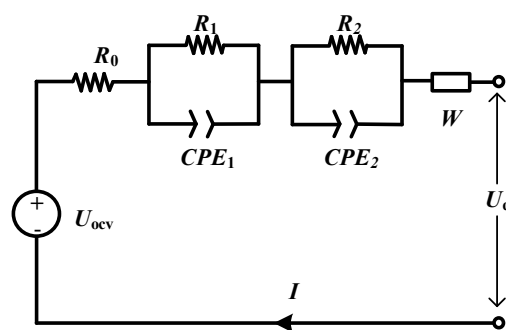
Figure 1. Schematic diagram of fractional-order equivalent circuit model.

In this circuit, the impedance of the fractional-order element can be described by the following equation:

$$\begin{cases} Z_{CPE_1} = \frac{1}{C_1 s^\alpha} \\ Z_{CPE_2} = \frac{1}{C_2 s^\beta} \\ Z_W = \frac{1}{W s^\gamma} \end{cases} \tag{1}$$

where, C_1, C_2, and W indicate the parameters of fractional-order elements; α and β represent the fractional order of CPE_1 and CPE_2 components. γ is the fractional order of the Warburg components.

The fractional differential equation of the parallel circuit of CPE and resistance can be expressed as:

$$D^\alpha U_{CPE_1}(t) = -\frac{1}{R_1 C_1} U_{CPE_1}(t) + \frac{1}{C_1} I(t) \tag{2}$$

$$D^\beta U_{CPE_2}(t) = -\frac{1}{R_2 C_2} U_{CPE_2}(t) + \frac{1}{C_2} I(t) \tag{3}$$

The fractional differential equation of the Warburg element is shown in Equation (4):

$$D^\gamma U_W(t) = -\frac{1}{W} I(t) \tag{4}$$

According to the definition, the system state of the SOC as a fractional-order model is presented in Equation (5) as follows:

$$D^1 SOC(t) = -\frac{\eta}{C_n} I(t) \tag{5}$$

where C_n is the battery rated capacity, η is the coulombic efficiency, and η is desirable 1 for lithium-ion batteries.

According to Kirchhoff's law of current and voltage, we obtain

$$U_d = U_{ocv} - I(t) R_0 - U_{CPE_1} - U_{CPE_2} - U_W \tag{6}$$

where U_{ocv} is the OCV of the battery, which is a monotonic function of the SOC.

In summary, the fractional-order equivalent circuit model of a lithium-ion battery can be established by Equations (1)–(6). A complex lithium-ion battery system can be described by the simple structure and limited parameters of the model. The parameters to be identified in the fractional model are shown in Equation (7), below:

$$\theta = [R_0 \ R_1 \ C_1 \ R_2 \ C_2 \ W \ \alpha \ \beta \ \gamma] \tag{7}$$

2.2. Lithium-Ion Battery Test Experiment

Battery test experiments are the premise of battery model establishment and state estimation, and are an indispensable step in battery research. In this paper, the battery test system is shown in Figure 2. The test object is a universal A123, ternary lithium-ion soft packet battery cell. The main parameters are listed in Table 1.
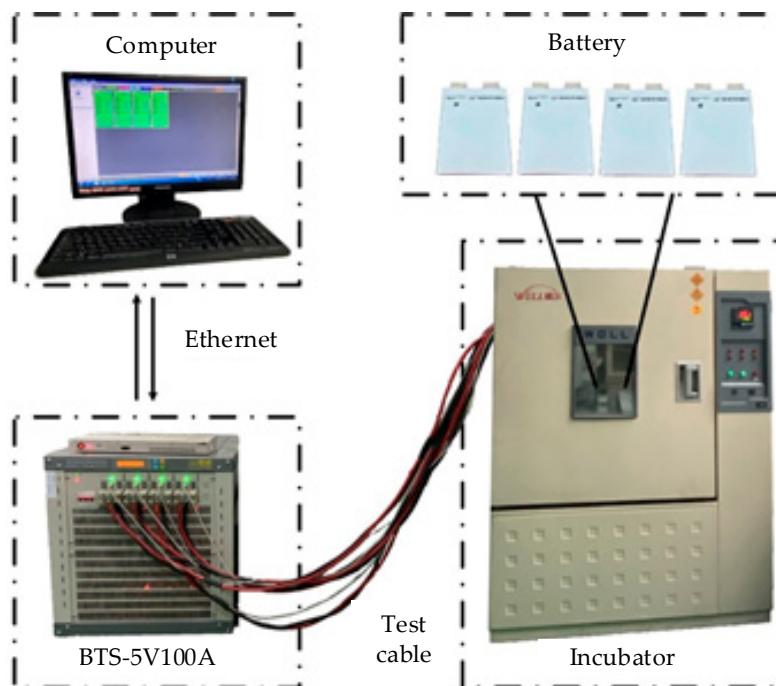
Figure 2. Software and hardware system for battery test experiment.

Table 1. Main performance parameters of universal A123 battery.

Nominal Capacity (Ah)	Nominal Voltage (V)	Charging Cut-Off Voltage (V)	Discharge Cut-Off Voltage (V)	Charging Cut-Off Current (A)
28	3.7	4.2	2.5	1.25

In order to identify the model parameters, a series of experiments on lithium-ion batteries were conducted with reference to relevant national standards and the USABC Electric Vehicle Battery Test Procedures Manual. The battery test flow chart of the relevant experiments is shown in Figure 3.
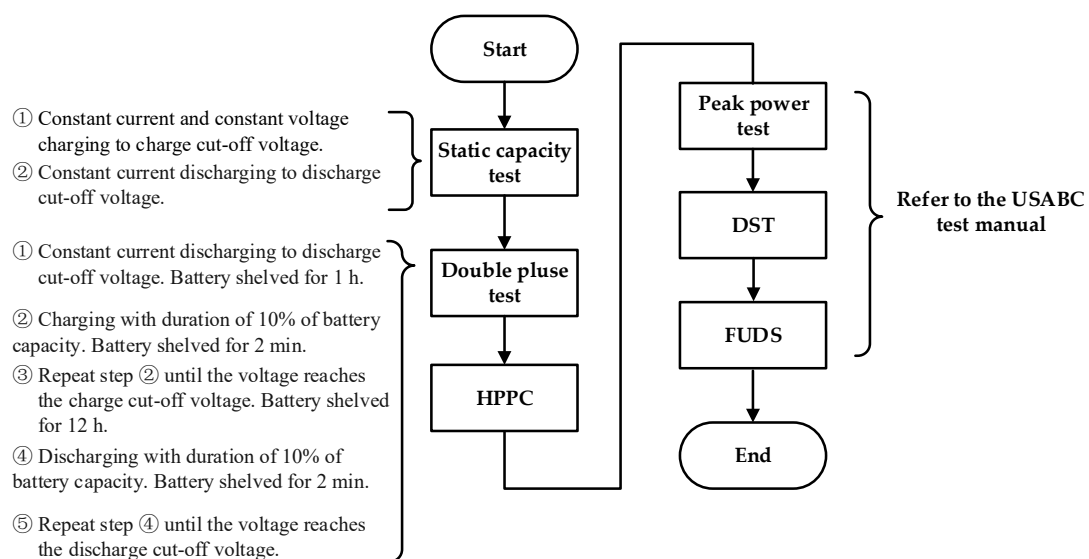

① Constant current and constant voltage charging to charge cut-off voltage.
② Constant current discharging to discharge cut-off voltage.

① Constant current discharging to discharge cut-off voltage. Battery shelved for 1 h.

② Charging with duration of 10% of battery capacity. Battery shelved for 2 min.

③ Repeat step ② until the voltage reaches the charge cut-off voltage. Battery shelved for 12 h.

④ Discharging with duration of 10% of battery capacity. Battery shelved for 2 min.

⑤ Repeat step ④ until the voltage reaches the discharge cut-off voltage.

Refer to the USABC test manual

Figure 3. Battery test flow chart.

According to the experimental data obtained by the double-pulse test, the relationship curve between OCV and SOC can be obtained by [33] using the empirical Equation (8), as shown in Figure 4.

$$U_{OCV}(SOC) = C_0 + C_1 SOC + C_2 \frac{1}{SOC} + C_3 \ln(SOC) + C_4 \ln(1 - SOC) \tag{8}$$
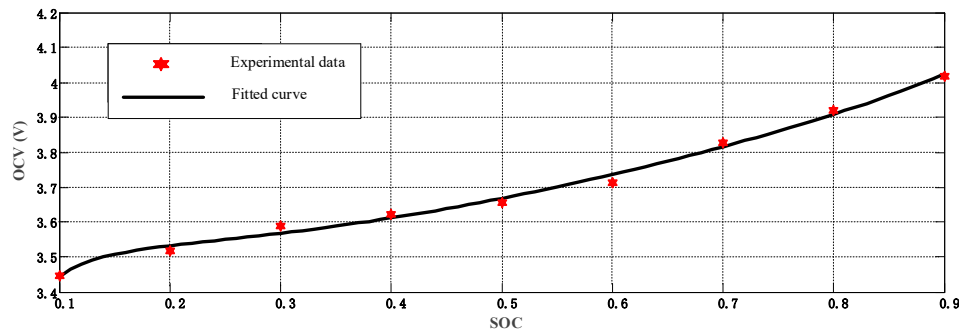
Figure 4. Open circuit voltage (OCV)–state of charge (SOC) fitting curve.

2.3. Model Parameter Identification Based on HPSO

The parameter identification link is very important before the model is successfully applied. The parameter identification results directly affect the accuracy of the model. Because of the obvious time-varying non-linear and complex structure of the lithium-ion battery system, there are many parameters involved in operation, and most parameter values cannot be directly measured. Therefore, parameter identification is a difficult problem in the battery modeling process. For high-dimensional complex optimization problems, this paper proposes an HPSO algorithm based on a genetic cross factor. The flowchart of the algorithm is shown in Figure 5.

Referring to the genetic algorithm (GA), the genetic crossover factor is introduced into the classic particle swarm optimization (PSO). After sorting the fitness of the particles from high to low, it is used to select the particles with the fitness of the top half in each generation. As part of the next generation of updated particle swarms, the particles in the second half of fitness are paired as crossover factors. The position of the exchange between the particles is called the intersection, which is randomly set. At the intersection point, the particles pair and exchange with each other to produce two completely new offspring. By comparing the fitness of the offspring particles with that of their parent particles and sorting them, the top half of the particles with high fitness values are selected to enter the next generation of updated particle swarm so as to realize the update of the particle swarm. The introduction of genetic crossover factors enriches the diversity of population particles, solves the problem that the classical PSO algorithm is prone to fall into the local optimality, improves the global searching capability of the parameter identification algorithm, and further improves the fitting degree of the battery model.
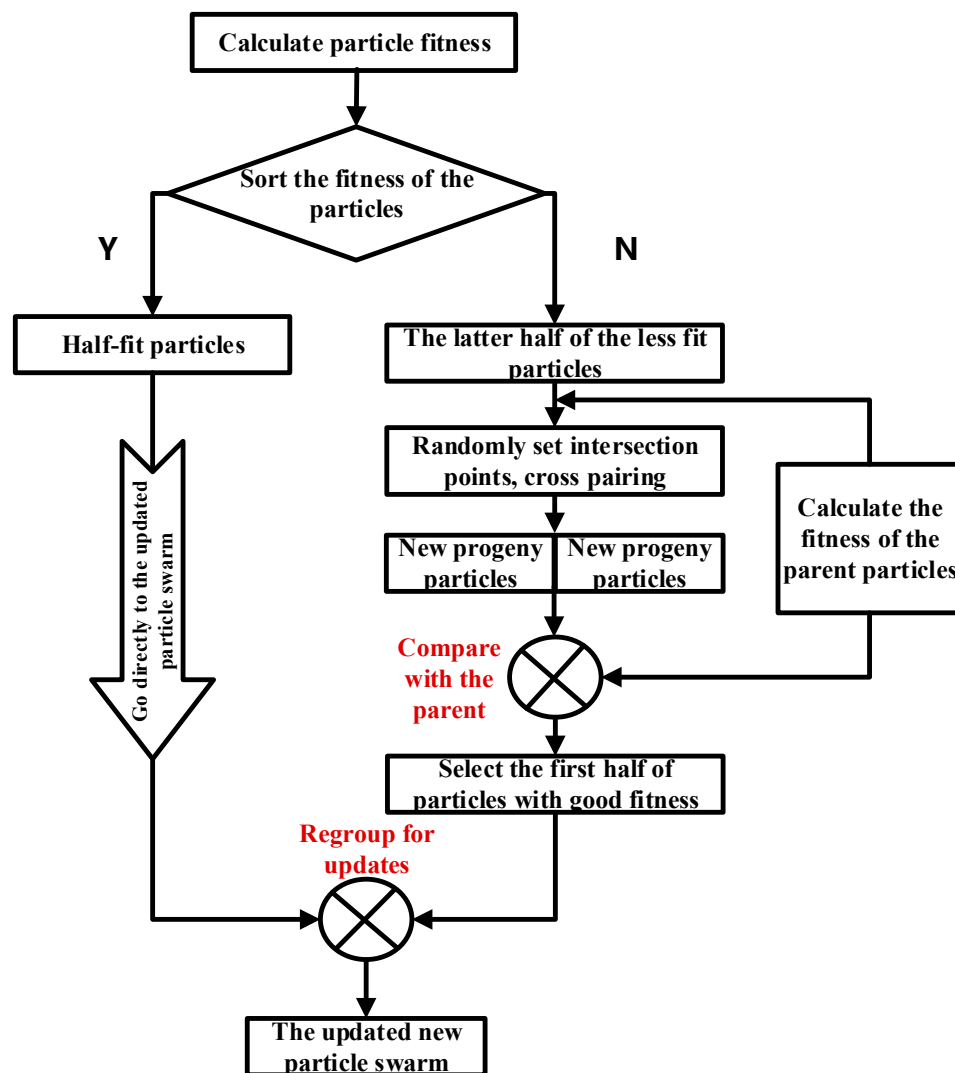
Figure 5. Flow chart of hybrid particle swarm filtering algorithm.

2.4. Fractional-Order Model Accuracy Analysis

In this selection, the dynamic stress test (DST) condition test data of the universal A123 battery at 25 °C ambient temperature is used as training data to identify the parameters of the established fractional-order model. Through different identification methods and different simulation conditions, the accuracy and robustness of the fractional-order model are analyzed.

The identification results obtained using the classical PSO algorithm are shown in Table 2.

Table 2. Parameter recognition results of ordinary particle swarm algorithm.

| R_0	R_1	C_1	R_2	C_2	W	A	β	γ
0.003	0.0001	960	7.12	1112	500	0.61	0.13	0.64

The identification results obtained using the HPSO algorithm are shown in Table 3.

Table 3. Parameter recognition results of hybrid particle swarm algorithm.

R_0	R_1	C_1	R_2	C_2	W	α	β	γ
0.001	0.05	5431	5.31	4758	2122	0.59	0.22	0.12

According to the identification results of the above two algorithms, the model accuracy is simulated and verified under the three working conditions of the dynamic stress test (DST), federal urban driving schedule (FUDS), and hybrid pulse power characteristic (HPPC). The simulation results are shown in Figures 6–8. It can be seen from Figures 6–8 that, under different operating conditions, the voltage error value output by the fractional-order model fluctuates slightly around zero. When the input current has a large mutation, the voltage error value is large, but can also be controlled at approximately 0.05 V. Therefore, the improved fractional-order model is more accurate and suitable for different working conditions.
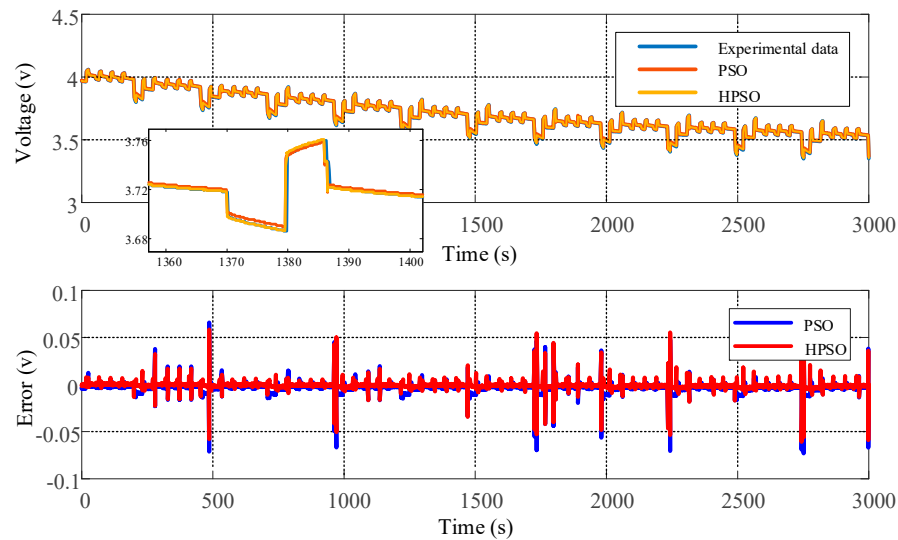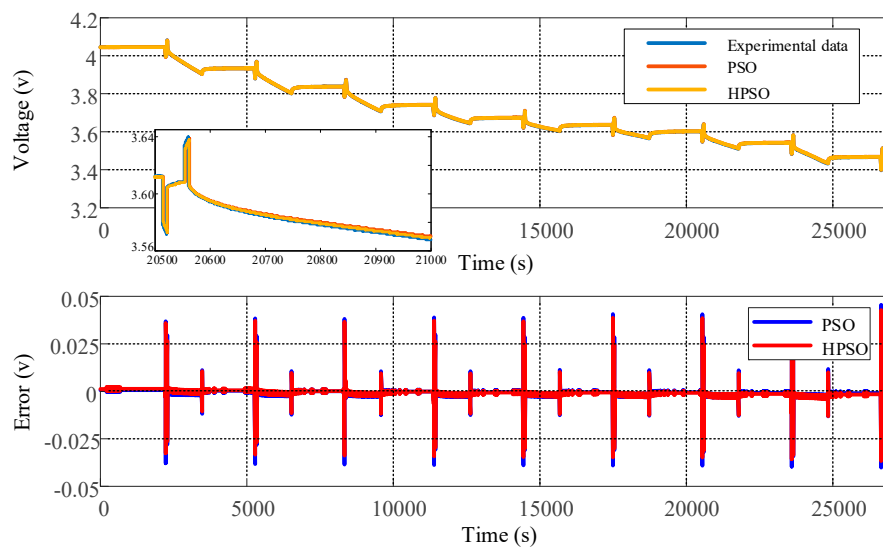

Figure 6. Model voltage and simulation error under dynamic stress test (DST) conditions.
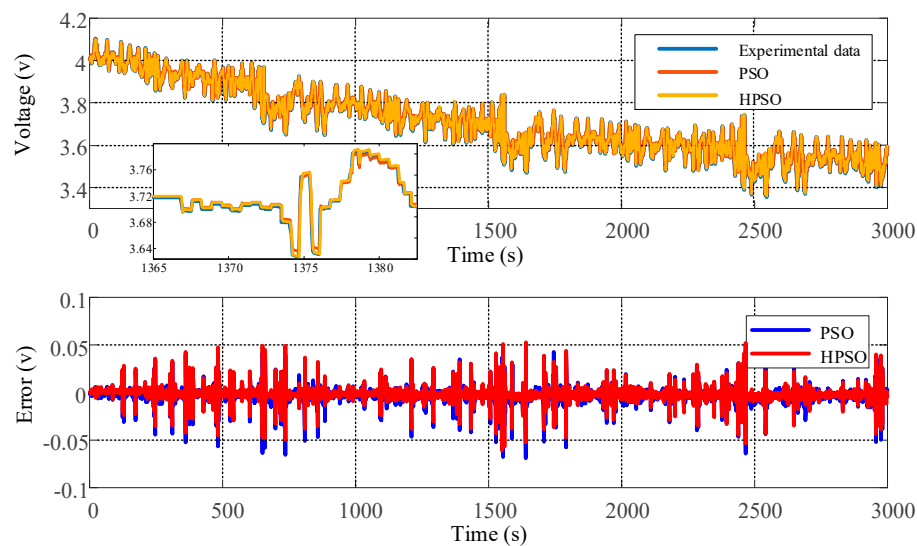
Figure 7. Model voltage and simulation error under federal urban driving schedule (FUDS) condition.

Figure 8. Model voltage and simulation error under hybrid pulse power characteristic (HPPC) conditions.

Table 4 shows the root mean square error (RMSE) value of the model output voltage corresponding to the classical PSO algorithm and the HPSO algorithm under different working conditions. It can be seen from Table 4 that the parameter identification method based on the HPSO algorithm further improved the accuracy of the fractional model.

Table 4. Root mean square error under different working conditions.

RMSE	HPPC	DST	FUDS
PSO	0.0061	0.0050	0.0057
HPSO	0.0036	0.0022	0.0035

3. SOC Estimation Based on the HIF Algorithm

The Kalman series of filtering algorithms have been supported, widely researched and applied owing to their high accuracy, low computational complexity, and good robustness. However, they have two limitations that are difficult to overcome: (1) It is necessary to ensure that the input noise is white noise, and the statistical characteristics of the noise are approximately known. In practice, the noise is often not a white noise that satisfies the Gaussian distribution, and the statistical characteristics are difficult to obtain. (2) The accuracy of the estimation is very dependent on the accuracy of the established model. When the accuracy of the model is insufficient or the accuracy of the model gradually decreases with the dynamic changes of the working process, the filtering error becomes increasingly larger.

To overcome the Kalman series filtering algorithm's requirements for white noise and its dependence on accurate modeling, an HIF with poor model accuracy, uncertain SOC initial value, and stronger robustness of various colored noise interference is introduced.

3.1. State Space Equation of the Lithium-Ion Battery

The establishment of system state space equations is the basis for controlling the parameters of dynamic systems in modern control theory. Establish a mathematical model that reflects the internal structure of the system and characterizes the system through the state equation and the output equation. Owing to the time-varying non-linearity of the battery system, its state space equation can be expressed as:

$$x_{k+1} = A_k x_k + B_k u_k + \omega_k \tag{9}$$

$$y_k = C_k x_k + D_k u_k + v_k \tag{10}$$

This is the first step in the derivation of the state space equation of a lithium-ion battery to determine the relevant variable parameters of the battery system. According to the established battery model, the state variable of the system is set as $x_k = [V_{CPE_1,k}\ V_{CPE_2,k}\ V_{W,k}\ SOC_k]$. The input of the system is $u = I_k$, which is the current state of the battery. The output is $y = U_{d,k}$, which is the terminal voltage of the battery.

After determining the parameters, according to the fractional-order model established in Section 2.1, the state space equations of Equations (8) and (9) are derived, where A_k, B_k, C_k, and D_k are defined as follows:

$$A_k = \begin{bmatrix} \alpha - T^\alpha \frac{1}{R_1 C_1} & 0 & 0 & 0 \\ 0 & \beta - T^\beta \frac{1}{R_2 C_2} & 0 & 0 \\ 0 & 0 & \gamma & 0 \\ 0 & 0 & 0 & 1 \end{bmatrix}, B_k = \begin{bmatrix} \frac{T^\alpha}{C_1} \\ \frac{T^\beta}{C_2} \\ -\frac{T^\gamma}{W} \\ -\frac{\eta T}{C_n} \end{bmatrix} \tag{11}$$

$$C_k = [-1\ -1\ -1\ \tfrac{df(SOC_k)}{dSOC}], D_k = -R_0$$

The implementation of SOC estimation is to design the corresponding filter algorithm based on the above-mentioned state space equations to eliminate the effects of noise ω_k and v_k as much as possible. With improvements in the accuracy of the system state estimation, the SOC estimation achieves the desired effect.

3.2. SOC Estimation Based on HIF Algorithm

To judge the accuracy of the estimated object x_k, the HIF algorithm defines a cost function J:

$$J = \frac{\sum\limits_{k=0}^{N-1} \|x_k - \hat{x}_k\|^2_{S_k}}{\|x_0 - \hat{x}_0\|^2_{P_0^{-1}} + \sum\limits_{k=0}^{N-1} (\|\omega_k\|^2_{Q_k^{-1}} + \|v_k\|^2_{R_k^{-1}})} \tag{12}$$

The matrices P_0, Q_k, R_k, and S_k in the equation are all symmetric positive definite matrices, which are set by the designer for specific problems. Designers use these matrices to reflect the degree to which different types of noise affect the system. In general, we expect to perform similar processing on the weights of different types of noises to avoid the impact on the accuracy of estimation when a certain type of noise is ignored.

It can be seen from Equation (11) that the cost function of HIF is a relative proportional value, and its numerator and denominator are related to the estimated value error and the overall noise of the system. The significance of establishing the cost function is to reflect the proportional relation between the estimation error and the noise interference. In order to meet the design requirements, the cost function has an upper bound, which satisfies the following condition:

$$J < 1/\theta$$

To solve the above optimization process, the algorithm designer must find a suitable x_k method to minimize the denominator of the cost function J. However, the reality is contrary to the designer's goal; it hopes to produce a specific special initialization state x_0, noise ω_k, and v_k, so as to maximize the cost function J.

Therefore, this problem becomes a maximum-minimum problem, that is, when ω_k, v_k, and x_0 make the cost function J maximum, the appropriate x_k should be selected to minimize the cost function

J. By re-integrating Equations (11) and (12) and combining it with the output Equation (9) of the state space, Equation (13) can be obtained:

$$-\frac{1}{\theta}\|x_0 - \hat{x}_0\|^2_{P_0^{-1}} + \sum_{k=0}^{N-1}\left[\|x_k - \hat{x}_k\|^2_{S_k} - \frac{1}{\theta}\left(\|\omega_k\|^2_{Q_k^{-1}} + \|y_k - C_k x_k - D_k u_k\|^2_{R_k^{-1}}\right)\right] < 0 \tag{13}$$

By solving the maximum-minimum problem of the cost function, a recursive relation satisfying Equation (12) can be obtained, as shown below:

$$\begin{cases} K_k = A_k P_k (I - \theta S_k P_k + C_k^T R_k^{-1} C_k P_k)^{-1} C_k^T R_k^{-1} \\ \hat{x}_{k+1} = A_k \hat{x}_k + B_k u_k + K_k(y_k - C_k \hat{x}_k - D_k u_k) \\ P_{k+1} = A_k P_k (I - \theta S_k + C_k^T R_k^{-1} C_k P_k)^{-1} A_k^T + Q_k \end{cases} \tag{14}$$

Similar to the KF algorithm, in order to facilitate calculation and application of the SOC estimation method based on the HIF, the recursive relation (Equation (14)) is divided into two stages: prediction and update. The specific calculation process is shown in Table 5.

Table 5. Battery SOC estimation algorithm based on H∞ filter algorithm.

The Specific Calculation Process Is as Follows:
Building a nonlinear system: $\begin{cases} x_k = f(x_{k-1}, u_{k-1}) + \omega_{k-1} \\ y_k = g(x_k, u_k) + v_k \end{cases}$
Initialization: $\hat{x}_0 = E(x_0), P_0^+ = E\left[(x_0 - \hat{x}_0)(x_0 - \hat{x}_0)^T\right]$
When $k \in \{1, 2, \ldots, \infty\}$, calculation
First step: prediction stage
System status estimation: $\hat{x}_k^- = f(\hat{x}_{k-1}^+, u_{k-1})$
Error covariance prediction: $P_k^- = A_{k-1} P_{k-1}^+ A_{k-1}^T + Q_{k-1}$
Second step: update stage
Innovation matrix: $e_k = y_k - g(\hat{x}_k^-, u_k)$
Gain matrix: $K_k = A_k P_k^- (I - \theta S_k P_k^- + C_k^T R_k^{-1} C_k P_k^-)^{-1} C_k^T R_k^{-1}$
System state correction: $\hat{x}_k^+ = \hat{x}_{k-1}^- K_k e_k$
Error covariance correction: $P_k^+ = A_k P_k^- (I - \theta S_k + C_k^T R_k^{-1} C_k P_k^-)^{-1} A_k^T + Q_k$

3.3. SOC Estimation Accuracy Verification

After describing in detail the principle of the HIF and the specific calculation process, in order to verify the robustness of the algorithm under the three conditions of uncertain measurement accuracy, initial SOC value uncertainty, and uncertain application conditions, this section uses a file in MATLAB software to write the HIF and EKF running procedures, and carries out simulation operations in Simulink. Based on the obtained experimental data, accuracy verification and comparative analysis are conducted on the estimation results of the SOC of the lithium-ion battery using HIF and EKF.

In the current literature, the reference values used for battery SOC estimation algorithm verification are all obtained by the ampere-hour integration method [34]. In order to eliminate the measurement error of the current sensor as far as possible, a high-precision battery testing equipment with a stability of 0.1% of FS is adopted, and the battery is fully placed before the test. Therefore, this study uses the approximate SOC calculation value obtained by the ampere-hour integration method as the real SOC value.

3.3.1. Uncertainty of Measurement Accuracy

Owing to the limitation of sensor acquisition accuracy, there are some acquisition errors in the current and voltage data acquired during vehicle driving. At present, the acquisition error of the mainstream current sensor is within 1%, and the voltage acquisition accuracy is within ±5 mV. In order

to fully ensure the reliability of the verification, this study evaluates the estimation effect of the HIF in the event of inaccurate measurement by adding colored noise interference to the current and voltage data.

Figure 9 shows that when colored noise is added to the current and voltage data, the SOC estimation results obtained by HIF and EKF have different degrees of deviation. Since the robustness of HIF algorithm is better than EKF, the SOC estimation results based on HIF are slightly better than that based on EKF. The estimation error of the former is within ±0.02, while that of the latter is within ±0.04.
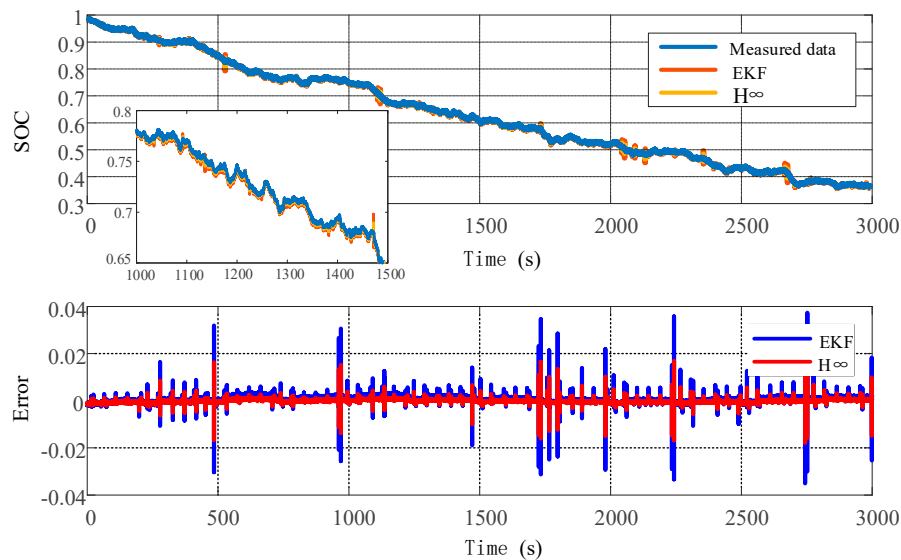
Figure 9. Comparison of SOC estimation results and errors based on DST conditions (colored noise added to current and voltage).

3.3.2. Uncertainty of SOC Initial Value

In actual use, it is difficult to obtain an accurate initial SOC value. Therefore, the algorithm should have the ability to track the system state when the initial SOC value is inaccurate, and correct the initial SOC value. To evaluate the convergence ability of the HIF under uncertain initial values, the initial value of the SOC is set to 0.7 (the exact initial value of the SOC is 1), and the results of its convergence curve and error are shown in Figure 10.

Figure 10 shows that in the case of the inaccurate initial SOC value, the SOC values estimated by the two algorithms can quickly converge to the accurate value after algorithm calculation. However, for the convergence rate, HIF needs approximately 1.5 s to make the SOC converge to the initial value, which is 50% higher than the 3 s of the EKF algorithm. Moreover, the estimated error of HIF fluctuates within ±0.02 after convergence, which proves that the algorithm is not sensitive to the setting of the initial value of SOC, can calculate the true value recursively, and has relatively better robustness.
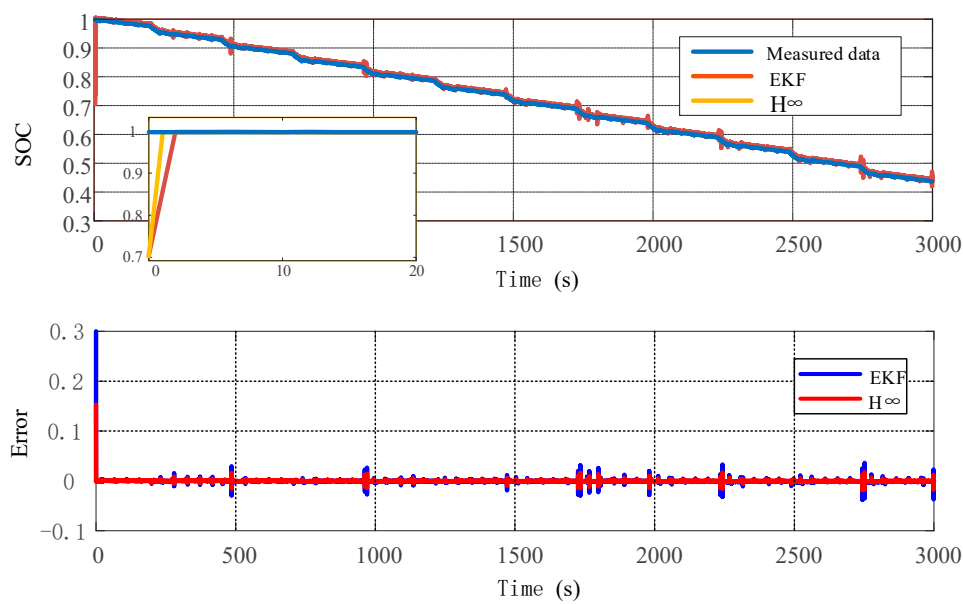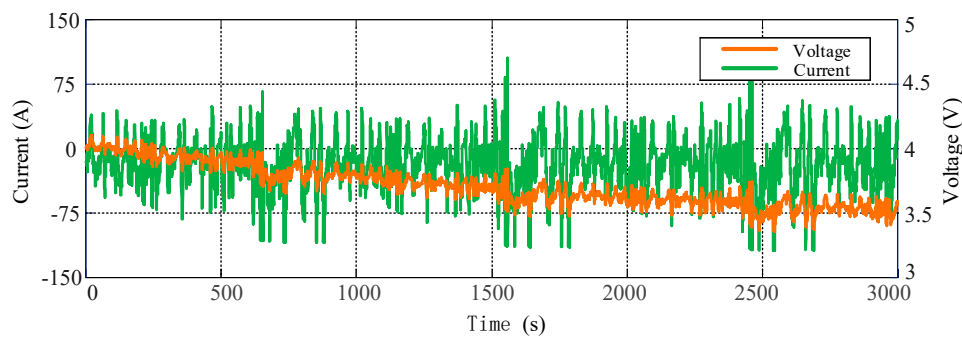
Figure 10. Comparison of SOC estimation results and errors under inaccurate SOC initial value based on DST conditions.

3.3.3. Uncertainty of Application Conditions

The applicability of the HIF algorithm under different operating conditions was evaluated using DST, FUDS, and HPPC conditions. It can be seen from Figures 11 and 12 that under DST and FUDS conditions, the current and voltage fluctuations are relatively severe. The noise interference of the battery model in this case is obvious, and it no longer exhibits the characteristics of zero mean. In addition, the model parameters change to a large extent with the current mutation. Figures 13 and 14 show that the EKF algorithm is used to estimate the battery SOC under the DST and FUDS conditions. The simulated output voltage of the battery model deviates greatly from the real voltage value, so that when the current pulse is large, the SOC estimation accuracy is not high, and fluctuates within ±0.04.
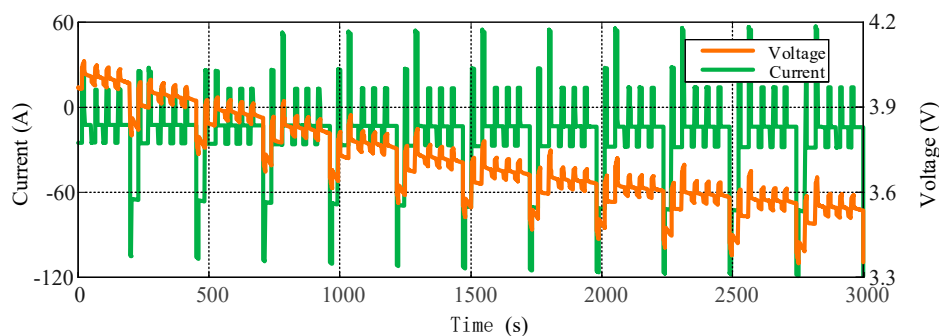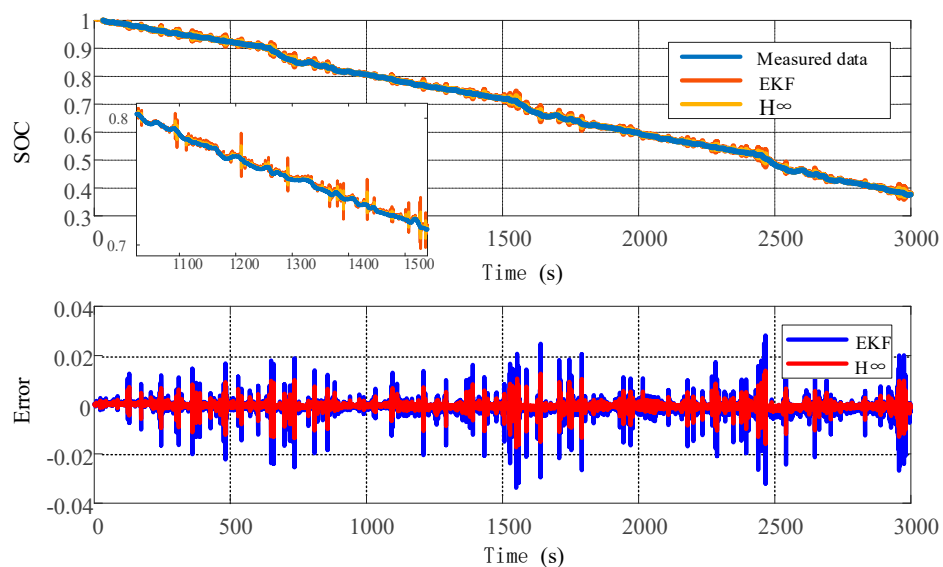

Figure 11. Current and voltage diagram under DST conditions.

Figure 12. Current and voltage diagram under FUDS condition.
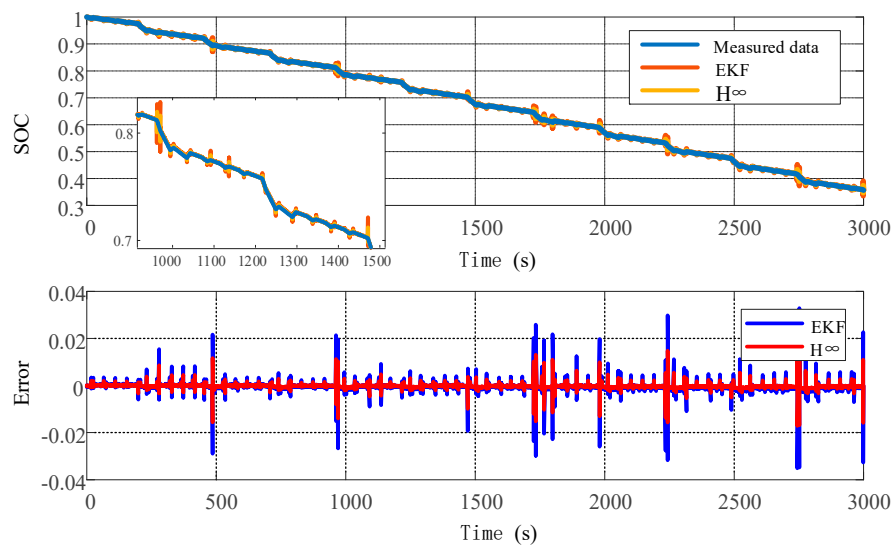
Figure 13. Comparison of SOC estimation results and errors under DST conditions.

Figure 14. Comparison of SOC estimation results and errors under FUDS conditions.

It can be seen from Figures 15 and 16 that the HPPC operating conditions are constant current pulse discharges, and the current fluctuates periodically. The HPPC condition is relatively stable, compared with the above two conditions, so the SOC estimation accuracy is relatively high. The SOC estimation error based on the EKF can be controlled within ±0.02, and the SOC estimation error based

on the HIF can be controlled within ±0.01, which further verifies the applicability of the HIF algorithm under different working conditions.
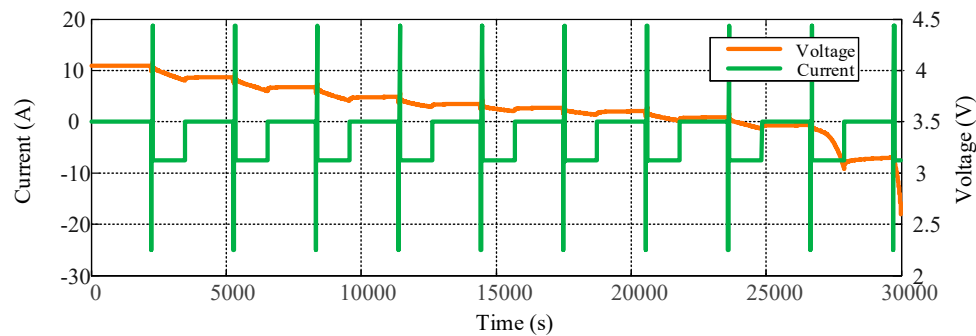

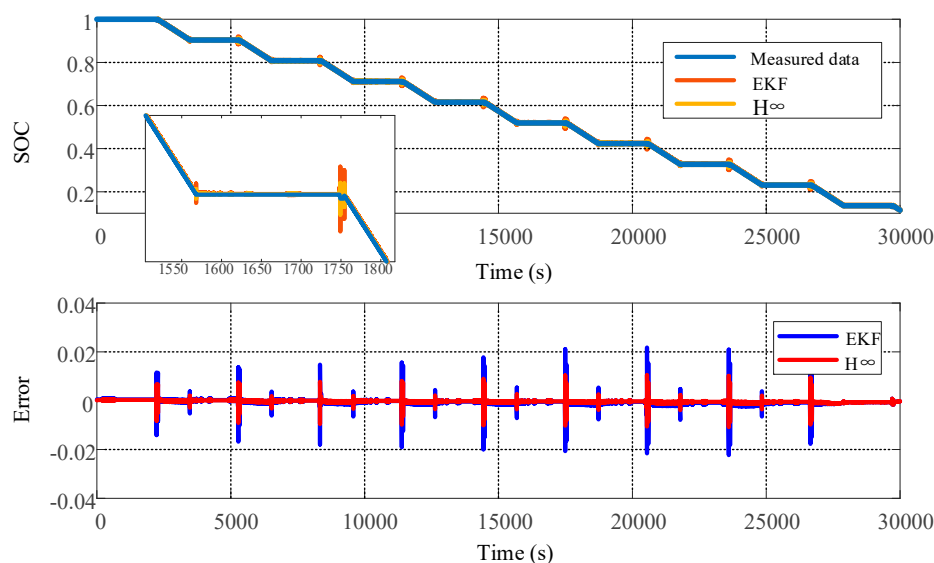**Figure 15.** Current–voltage diagram under HPPC conditions.

Figure 16. Comparison of SOC estimation results and errors under HPPC conditions.

4. Conclusions

Aiming at the SOC estimation problem of electric vehicle power lithium-ion batteries, this paper proposes an SOC estimation method based on the HIF algorithm. Firstly, based on the EIS of the lithium-ion battery, a fractional-order model based on the dual polarization equivalent circuit model was established. Without reducing the accuracy of the model, it not only simplifies the model structure, but also reduces the amount of calculation. Then, the parameters of the fractional-order battery model are identified by the HPSO algorithm based on the genetic crossover factor. It solves the problem that the classic PSO algorithm easily falls into the local best, improves the global search ability of the parameter identification algorithm, and further improves the fitting degree of the battery model. Finally, the accuracy of the SOC estimation results of lithium-ion batteries using HIF and EKF are verified and compared under three conditions: uncertain measurement accuracy, uncertain SOC initial value, and uncertain application conditions. The simulation results show that the SOC estimation method based on HIF can ensure that the SOC estimation error value fluctuates within ±0.02 in any case, and is slightly affected by environmental factors and other factors. It provides a way to improve the accuracy of SOC estimation in a battery management system.

Abbreviations

SOC	state of charge
HIF	H-infinity filter
HPSO	hybrid particle swarm optimization
EKF	extended Kalman filter
OCV	open circuit voltage
EIS	electrochemical impedance spectroscopy
SVM	support vector machine
NN	neural network
PF	particle filter
KF	Kalman filter
AUKF	adaptive unscented Kalman filter
AHIF	adaptive H-infinity filter
CPE	constant phase element
GA	genetic algorithm
DST	dynamic stress test
FUDS	federal urban driving schedule
HPPC	hybrid pulse power characteristic
RMSE	root mean square error

References

1. Xiong, R.; Cao, J.; Yu, Q.; He, H.; Sun, F. Critical review on the battery state of charge estimation methods for electric vehicles. *IEEE Access* **2018**, *6*, 1832–1843. [CrossRef]
2. Chaoui, H.; Ibe-Ekeocha, C.C. State of charge and state of health estimation for lithium batteries using recurrent neural networks. *IEEE Trans. Veh. Technol.* **2017**, *66*, 8773–8783. [CrossRef]
3. Lin, C.; Mu, H.; Xiong, R.; Shen, W. A novel multi-model probability battery state of charge estimation approach for electric vehicles using h-infinity algorithm. *Appl. Energy* **2016**, *166*, 76–83. [CrossRef]
4. Zheng, Y.; Ouyang, M.; Han, X.; Lu, L.; Li, J. Investigating the error sources of the online state of charge estimation methods for lithium-ion batteries in electric vehicles. *J. Power Sources* **2018**, *377*, 161–188. [CrossRef]
5. Einhorn, M.; Conte, F.V.; Kral, C.; Fleig, J. A method for online capacity estimation of lithium ion battery cells using the state of charge and the transferred charge. *IEEE Trans. Ind. Appl.* **2011**, *48*, 736–741. [CrossRef]
6. Li, Z.; Huang, J.; Liaw, B.; Zhang, J. On state-of-charge determination for lithium-ion batteries. *J. Power Sources* **2017**, *348*, 281–301. [CrossRef]
7. Hannan, M.A.; Lipu, M.S.H.; Hussain, A.; Mohamed, A. A review of lithium-ion battery state of charge estimation and management system in electric vehicle applications: Challenges and recommendations. *Renew. Sustain. Energy Rev.* **2017**, *78*, 834–854. [CrossRef]
8. Salkind, A.J.; Fennie, C.; Singh, P.; Atwater, T.; Reisner, D.E. Determination of state-of-charge and state-of-health of batteries by fuzzy logic methodology. *J. Power Sources* **1999**, *80*, 293–300. [CrossRef]
9. Jin, G.; Li, L.; Xu, Y.; Hu, M.; Fu, C.; Qin, D. Comparison of SOC estimation between the integer-order model and fractional-order model under different operating conditions. *Energies* **2020**, *13*, 1785. [CrossRef]

10. Gupta, D.; Richhariya, B.; Borah, P. A fuzzy twin support vector machine based on information entropy for class imbalance learning. *Neural Comput. Appl.* **2018**, *31*, 7153–7164. [CrossRef]

11. Herzog, S.; Tetzlaff, C.; Wörgötter, F. Evolving artificial neural networks with feedback. *Neural Networks* **2020**, *123*, 153–162. [CrossRef] [PubMed]

12. Lv, M.; Baldi, S.; Liu, Z. The non-smoothness problem in disturbance observer design: A set-invariance-based adaptive fuzzy control method. *IEEE Trans. Fuzzy Syst.* **2019**, *27*, 598–604. [CrossRef]

13. Yang, Q.; Cao, B.; Li, X. A simplified fractional order impedance model and parameter identification method for lithium-ion batteries. *PLoS ONE* **2017**, *12*, e0172424. [CrossRef] [PubMed]

14. Ma, Y.; Chen, Y.; Zhou, X.; Chen, H. Remaining useful life prediction of lithium-ion battery based on gauss–hermite particle filter. *IEEE Trans. Control. Syst. Technol.* **2019**, *27*, 1788–1795. [CrossRef]

15. Li, R.; Jan, N.M.; Huang, B.; Prasad, V. Constrained multimodal ensemble Kalman filter based on Kullback–Leibler (KL) divergence. *J. Process. Control.* **2019**, *79*, 16–28. [CrossRef]

16. Waag, W.; Fleischer, C.; Sauer, D.U. Critical review of the methods for monitoring of lithium-ion batteries in electric and hybrid vehicles. *J. Power Sources* **2014**, *258*, 321–339. [CrossRef]

17. Sun, F.; Xiong, R.; He, H. A systematic state-of-charge estimation framework for multi-cell battery pack in electric vehicles using bias correction technique. *Appl. Energy* **2016**, *162*, 1399–1409. [CrossRef]

18. Wang, T.; Chen, S.; Ren, H.; Zhao, Y. Model-based unscented Kalman filter observer design for lithium-ion battery state of charge estimation. *Int. J. Energy Res.* **2017**, *42*, 1603–1614. [CrossRef]

19. Cui, X.; He, Z.; Li, E.; Cheng, A.; Luo, M.; Guo, Y. State-of-charge estimation of power lithium-ion batteries based on an embedded micro control unit using a square root cubature Kalman filter at various ambient temperatures. *Int. J. Energy Res.* **2019**, *43*, 3561–3577. [CrossRef]

20. Xiong, B.; Zhao, J.; Wei, Z.; Skyllas-Kazacos, M. Extended Kalman filter method for state of charge estimation of vanadium redox flow battery using thermal-dependent electrical model. *J. Power Sources* **2014**, *262*, 50–61. [CrossRef]

21. Shen, P.; Ouyang, M.; Lu, L.; Li, J.; Feng, X. The co-estimation of state of charge, state of health, and state of function for lithium-ion batteries in electric vehicles. *IEEE Trans. Veh. Technol.* **2018**, *67*, 92–103. [CrossRef]

22. Wang, L.; Lu, N.; Liu, Q.; Liu, L.; Zhao, X. State of charge estimation for lifepo4 battery via dual extended kalman filter and charging voltage curve. *Electrochim. Acta* **2019**, *296*, 1009–1017. [CrossRef]

23. Plett, G.L. Extended Kalman filtering for battery management systems of lipb-based hev battery packs part 1. background. *J. Power Sources* **2004**, *134*, 262–276. [CrossRef]

24. Plett, G.L. Sigma-point Kalman filtering for battery management systems of lipb-based hev battery packs. *J. Power Sources* **2006**, *161*, 1356–1368. [CrossRef]

25. Sun, F.; Xiong, R. A novel dual-scale cell state-of-charge estimation approach for series-connected battery pack used in electric vehicles. *J. Power Sources* **2015**, *274*, 582–594. [CrossRef]

26. Chen, N.; Zhang, P.; Dai, J.; Gui, W. Estimating the state-of-charge of lithium-ion battery using an h-infinity observer based on electrochemical impedance model. *IEEE Access* **2020**, *8*, 26872–26884. [CrossRef]

27. Shu, X.; Li, G.; Shen, J.; Yan, W.; Chen, Z.; Liu, Y. An adaptive fusion estimation algorithm for state of charge of lithium-ion batteries considering wide operating temperature and degradation. *J. Power Sources* **2020**, *462*, 228132. [CrossRef]

28. Gong, X.; Suh, J.; Lin, C. A novel method for identifying inertial parameters of electric vehicles based on the dual h infinity filter. *Veh. Syst. Dyn.* **2019**, *58*, 28–48. [CrossRef]

29. Xiong, W.; Mo, Y.; Yan, C. Lithium-ion battery parameters and state of charge joint estimation using bias compensation least squares and the alternate algorithm. *Math. Probl. Eng.* **2020**, *2020*, 1–16. [CrossRef]

30. Xu, W.; Xu, J.; Lang, J.; Yan, X. A multi-timescale estimator for lithium-ion battery state of charge and state of energy estimation using dual h infinity filter. *IEEE Access* **2019**, *7*, 181229–181241. [CrossRef]

31. Zhang, Q.; Shang, Y.; Li, Y.; Cui, N.; Duan, B.; Zhang, C. A novel fractional variable-order equivalent circuit model and parameter identification of electric vehicle li-ion batteries. *ISA Trans.* **2020**, *97*, 448–457. [CrossRef] [PubMed]

32. Wang, Q.; He, Y.-J.; Shen, J.-N.; Hu, X.; Ma, Z.-F. State of charge-dependent polynomial equivalent circuit modeling for electrochemical impedance spectroscopy of lithium-ion batteries. *IEEE Trans. Power Electron.* **2017**, *33*, 8449–8460. [CrossRef]

33. Lin, X.; Perez, H.E.; Mohan, S.; Siegel, J.B.; Stefanopoulou, A.G.; Ding, Y.; Castanier, M.P. A lumped-parameter electro-thermal model for cylindrical batteries. *J. Power Sources* **2014**, *257*, 1–11. [CrossRef]
34. Xu, Z.; Gao, S.; Yang, S. Lifepo4 battery state of charge estimation based on the improved thevenin equivalent circuit model and Kalman filtering. *J. Renew. Sustain. Energy* **2016**, *8*, 24103. [CrossRef]